Supporting Information for:

Improving efficiency and stability of colorful perovskite solar cells with two-dimensional photonic crystals

Zhou Liu[†], Longlong Wu[†], Xiao Wang[†], Qiaofei Xu[†], Youdi Hu[†], Ke Meng[†], and Gang Chen[†,^*]*

[†]School of Physical Science and Technology, ShanghaiTech University, Shanghai, China 201210

[^]Shanghai Synchrotron Radiation Facility, Shanghai Institute of Applied Physics, Chinese Academy of Sciences, Shanghai, China 201204

[*]E-mail: gchen@shanghaitech.edu.cn (G.C.); mengke@shanghaitech.edu.cn (K.M.)

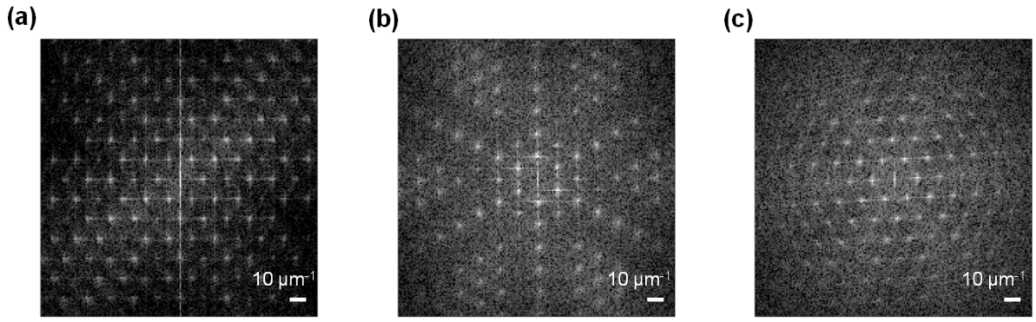

Figure S1. Fourier transform patterns of the SEM images of (a) PS template, (b) IOS, (c) IOST.

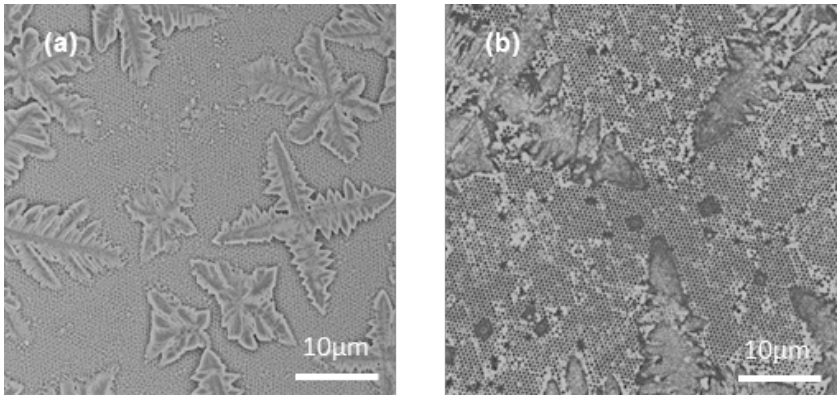

Figure S2. SEM images of the IOS films fabricated at the spin speed of (a) 3000 rpm and (b) 7000 rpm, respectively.

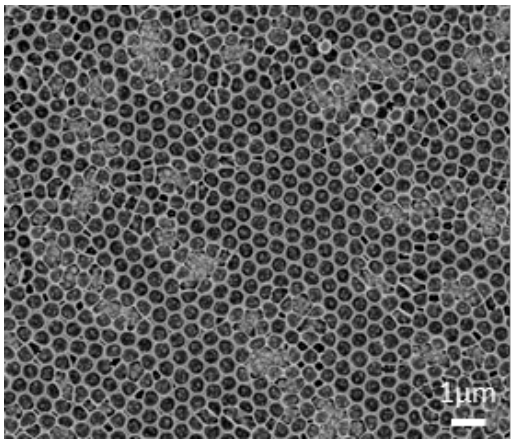

Figure S3. SEM image of the IOS film fabricated at the high ramp speed of temperature.

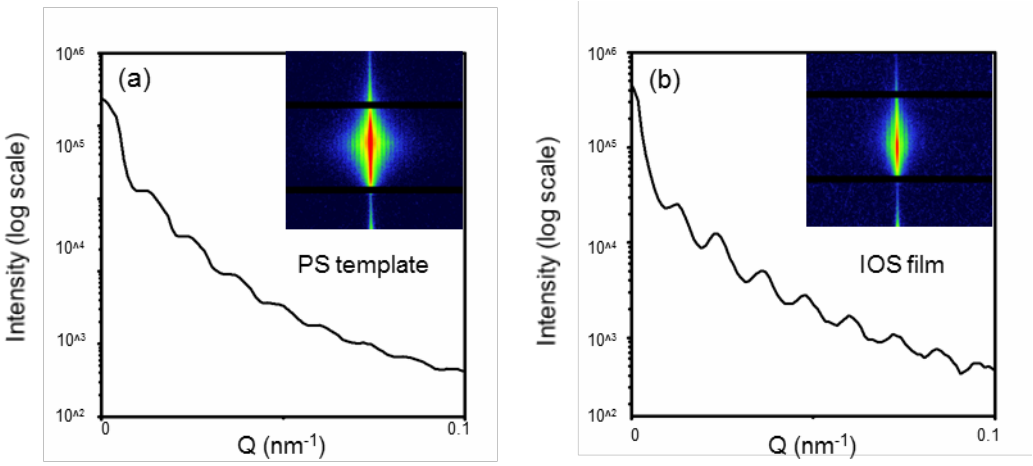

Figure S4. GISAXS curves of (a) the PS template and (b) the IOS film. Insets show the corresponding 2D GISAXS images.

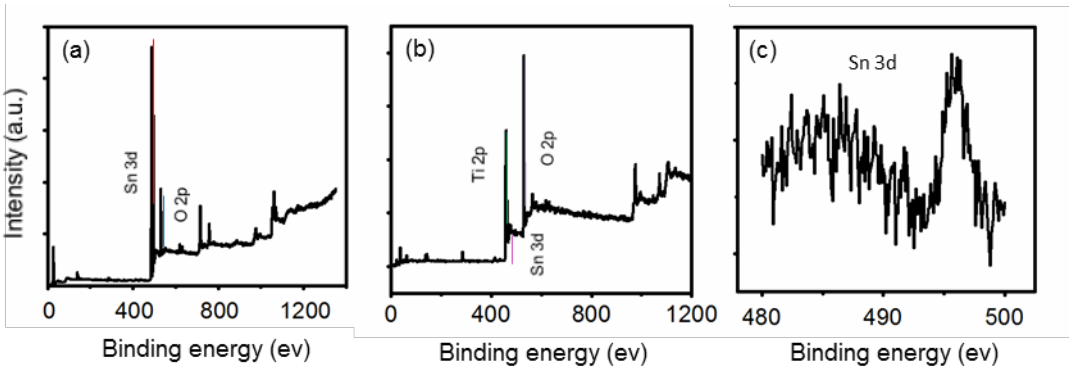

Figure S5. XPS surveys of (a) the IOS film and (b) the IOST film. (c) Zoom-in XPS spectrum of the IOST film in the Sn 3d region.

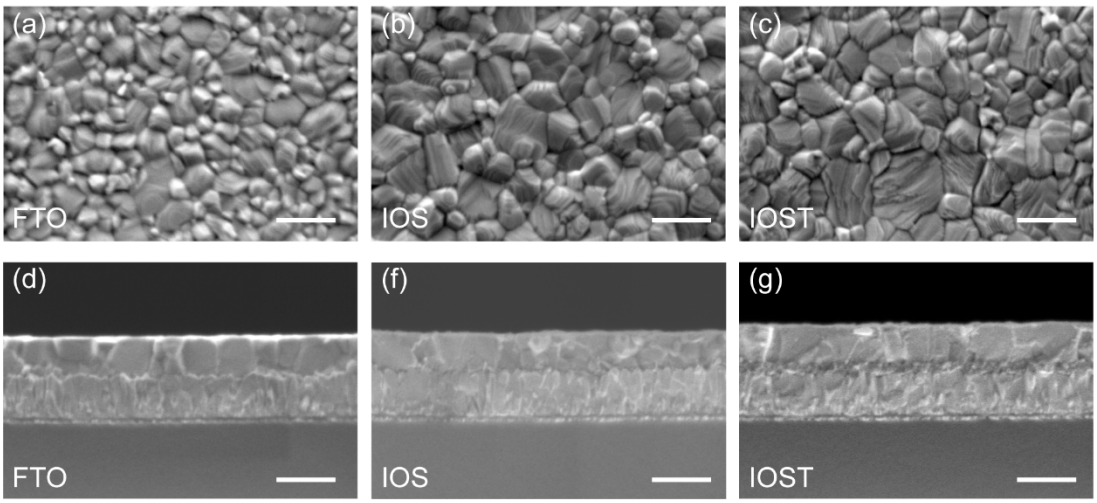

Figure S6. The top-view and cross-sectional SEM images of the perovskite films based on different substrates: (a), (d) FTO, (b), (f) IOS and (c), (g) IOST. The scale bars are 500 nm.

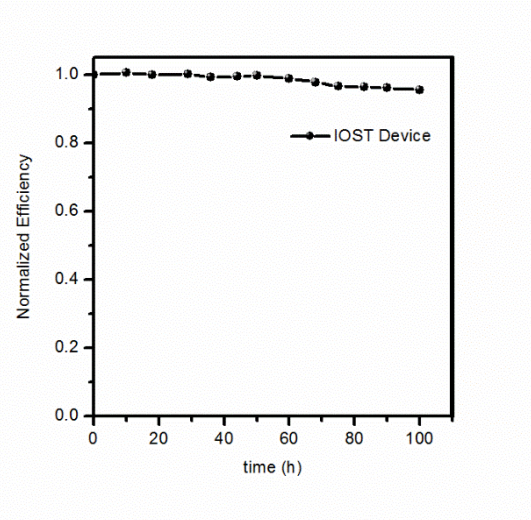

Figure S7. Stability test of the IOST based solar cell device (cells were stored and characterized in a N_2 filled glovebox).

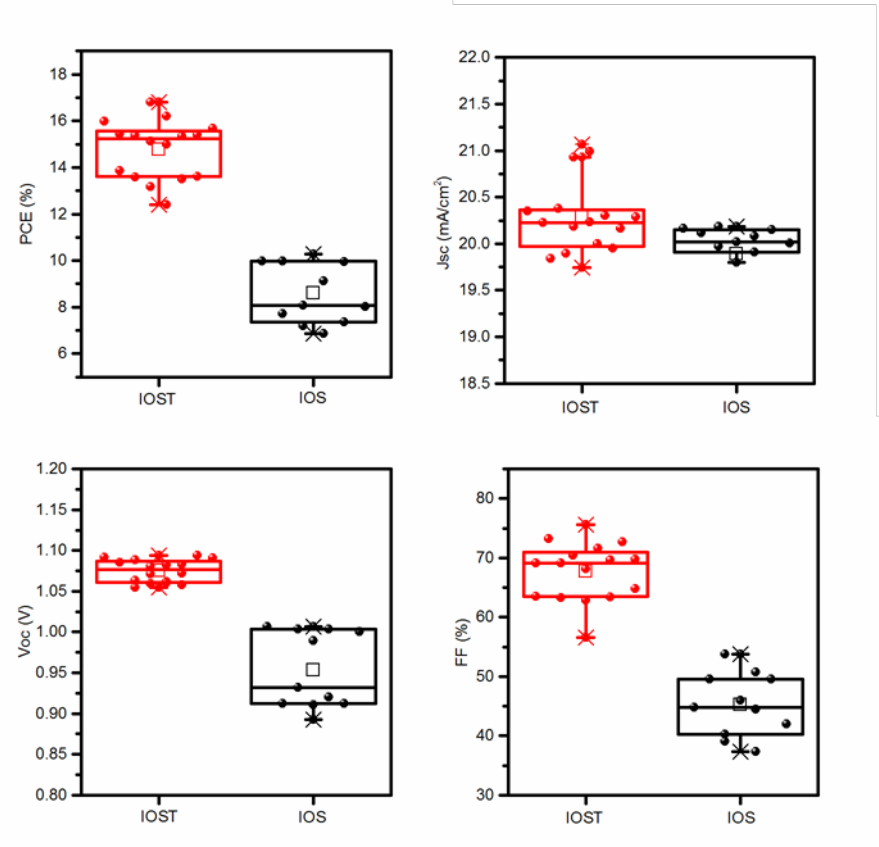

Figure S8. Photovoltaic parameters distribution of 15 cells based on IOS and IOST.

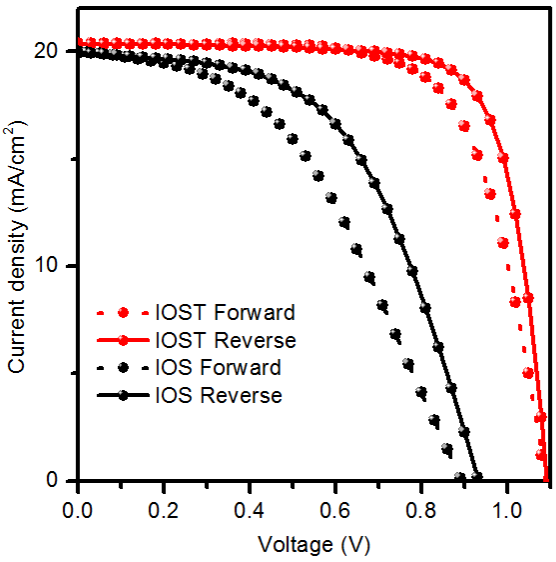

Figure S9. *J-V* reverse (from 1.2 to 0 V) and forward (from 0 to 1.2 V) scan results of IOS and IOST based PSCs.

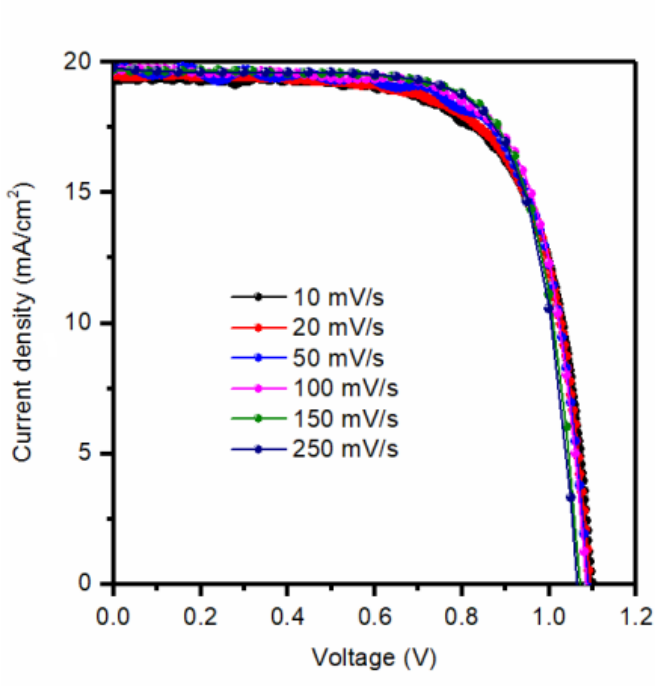

Figure S10. Scan rate dependence of the J-V characteristics of the IOST based PSCs.

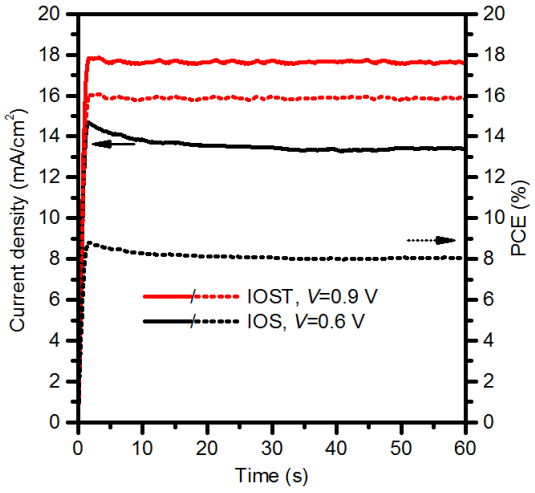

Figure S11. Stabilized photocurrent and maximum power point tracking results of the IOS and IOST based PSCs.

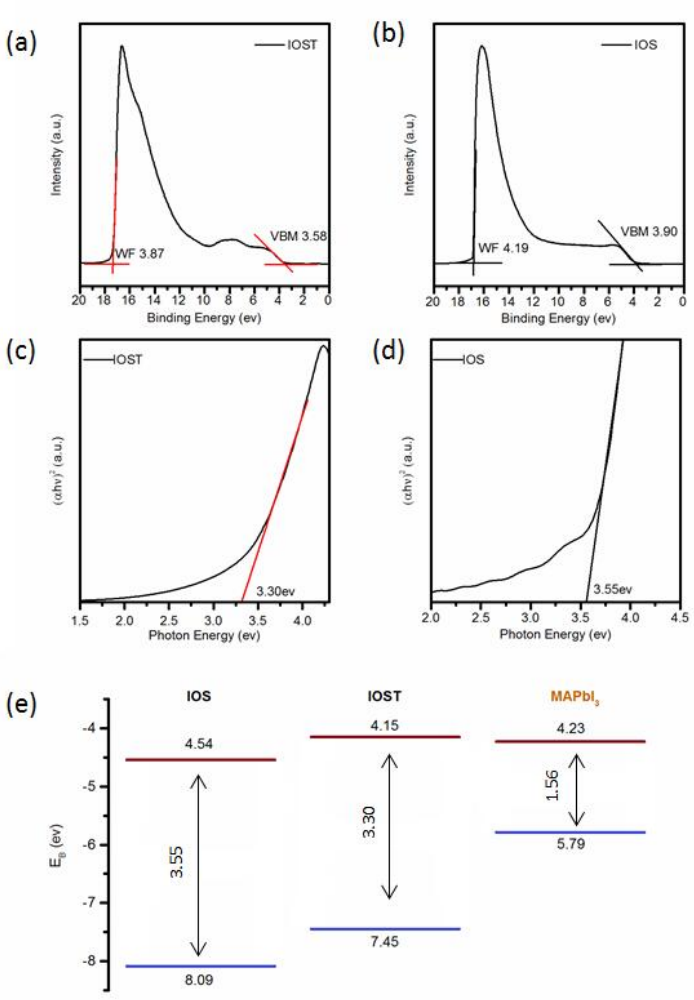

Figure S12. UPS spectra (He I) of the (a) IOST and (b) IOS ETLs. Tauc plots of the (c) IOST and (d) IOS ETLs. (e) Schematic conduction band diagrams of the $MAPbI_3$ perovskite films and the electron transporting layers.

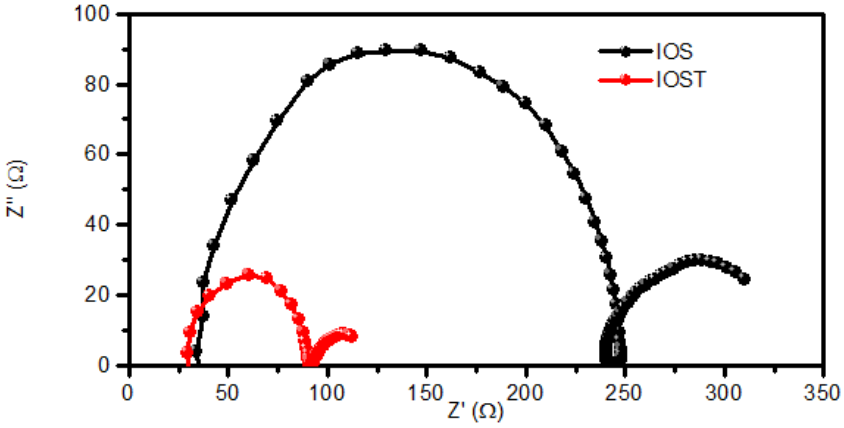

Figure S13. Nyquist plots of the devices based on IOS and IOST (cells measured at the open circuit voltage under 1 sun illumination).

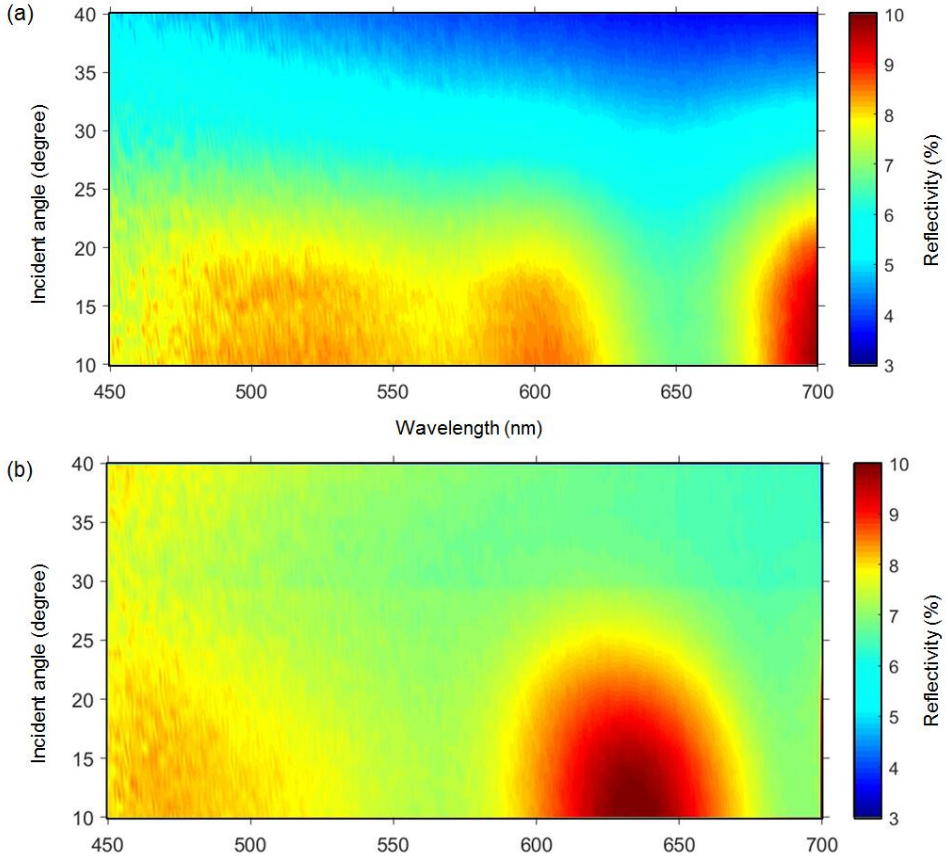

Figure S14. Variable-angle reflection spectra of the (a) IOST and (b) planar TiO_2 thin film based PSC device.

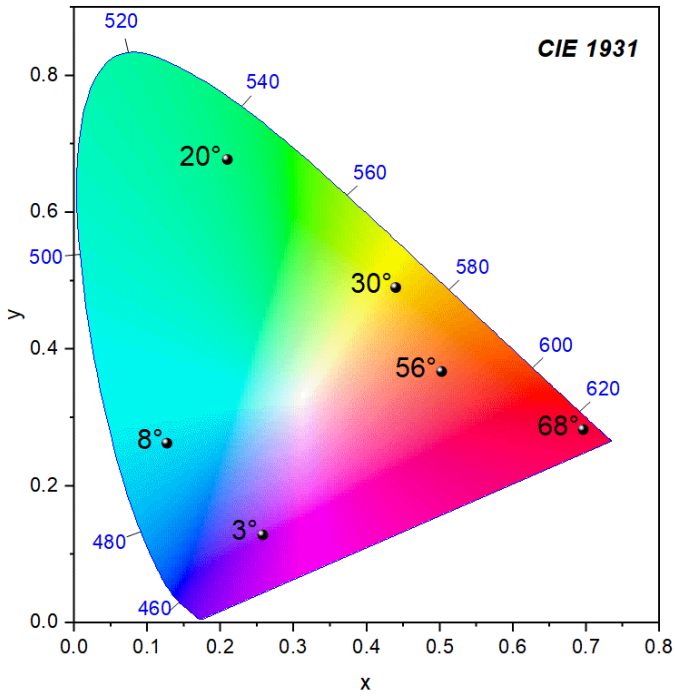

Figure S15. On the CIE 1931 chromaticity space, the color hues of the IOST-based perovskite films are calculated for the typical light incidence angles between 0º and 80º with respect to the surface normal.